Exp Brain Res (2009) 197:101–109
DOI 10.1007/s00221-009-1896-0

RESEARCH ARTICLE

Differential expression of two glutamate transporters, GLAST and GLT-1, in an experimental rat model of glaucoma

Chan Kee Park · Jiook Cha · Soo Chul Park · Phil Young Lee · Jie Hyun Kim · Hwa Sun Kim · Shin Ae Kim · In-Beom Kim · Myung-Hoon Chun

Received: 24 November 2008 / Accepted: 4 June 2009 / Published online: 24 June 2009

Abstract Glutamate is the major excitatory neurotransmitter of the mammalian retina, and excessive glutamate has been implicated in the pathogenesis of glaucoma. It is well known that glutamate transport, mainly *via* GLAST and GLT-1, is cardinal mechanism for maintaining glutamate homeostasis in normal and pathological conditions, including ischemia in the brain. In an effort to understand the role of glutamate and the glutamate regulation system of the retina in the pathogenesis of glaucoma, we examined changes in the expression of two glutamate transporters, GLAST and GLT-1, by Western blot analysis and immunocytochemistry in a rat glaucoma model. GLT-1 was expressed in cone photoreceptors and some cone bipolar cells and the levels of expression were significantly increased in the cauterized eyes throughout the entire experimental period. In contrast, GLAST expression, which occurred in Müller cells, the main retinal glial cells, remained stable during the experimental period. These results suggest that GLT-1 may be a prerequisite for the maintenance of glutamate homeostasis in the retina undergoing glaucoma.

C. K. Park · S. C. Park · P. Y. Lee · J. H. Kim · H. S. Kim
Department of Ophthalmology, College of Medicine,
The Catholic University of Korea, 505 Banpo-dong,
Socho-gu, Seoul 137-701, Korea

J. Cha · S. A. Kim · I.-B. Kim (✉) · M.-H. Chun (✉)
Department of Anatomy, College of Medicine,
The Catholic University of Korea, 505 Banpo-dong,
Socho-gu, Seoul 137-701, Korea
e-mail: ibkimmd@catholic.ac.kr

M.-H. Chun
e-mail: mhchun@catholic.ac.kr

Keywords Retina · Glaucoma · Glutamate transporters · GLAST · GLT-1 · Animal model

Abbreviations

EAAT	Excitatory amino acid transporter
GCL	Ganglion cell layer
INL	Inner nuclear layer
IOP	Intraocular pressure
IPL	Inner plexiform layer
ONL	Outer nuclear layer
OPL	Outer plexiform layer
PB	Phosphate buffer
PBS	Phosphate buffered saline
PMSF	Phenylmethylsulfonyl fluoride
RGC	Retinal ganglion cell

Introduction

Glutamate is a major excitatory neurotransmitter in the brain and retina, and its uptake is essential for normal transmission at the glutamatergic synapses (Danbolt 2001; Massey and Miller 1990). Under physiological conditions, glutamate transporters expressed in glial cells and neurons of the retina move extracellular glutamate rapidly into the intracellular space, thus maintaining a low extracellular glutamate concentration (Pow and Barnett 2000; Rauen et al. 1998). High levels of extracellular glutamate are excitotoxic to the neuronal cells and have been implicated in the pathogenesis of many brain diseases, including stroke, trauma, epilepsy, and dementia (Maragakis and Rothstein 2001; Rothstein et al. 1992).

To date, five distinct excitatory amino acid transporters (EAATs) that transport glutamate have been cloned: GLAST (Storck et al. 1992), GLT-1 (Pines et al. 1992),

EAAC1 (Kanai and Hediger 1992), EAAT4 (Fairman et al. 1995) and EAAT5 (Arriza et al. 1997). GLAST and GLT-1, which are exclusively located in glial cells in the brain (Danbolt et al. 1992; Lehre et al. 1995, 1997; Levy et al. 1993), are also present in the retina. In the mammalian retina, GLAST is considered to be the major glutamate transporter and is expressed in Müller cells (Izumi et al. 2002; Pow 2001; Rauen 2000; Rauen et al. 1996, 1998), the main glial cells in the retina, while GLT-1, which is known to be responsible for up to 90% of all glutamate transport in the forebrain region (Robinson 1998), is found in retinal neurons, such as cone photoreceptors and certain types of cone bipolar cells (Pow 2001; Rauen 2000; Rauen et al. 1996). To our knowledge, little appears to be known concerning the functional significance of GLT-1 expression in these retinal neurons.

Elevated levels of glutamate have been reported in the vitreous of glaucomatous eyes in humans and monkeys (Dreyer et al. 1996). A reduction in the level of GLAST has been reported in a rat glaucoma model (Martin et al. 2002), a mouse glaucoma model (Schuettauf et al. 2007), and in human glaucoma (Naskar et al. 2000). In addition, GLT-1, the main neuronal glutamate transporter in the retina, is down-regulated in glaucomatous eyes in rats (Martin et al. 2002) and mice (Schuettauf et al. 2007). However, several studies have not been able to replicate these findings. That is, GLAST expression is increased in a laser-induced chronic rat glaucoma model (Woldemussie et al. 2004), and the evoked expression of GLT-1c, a GLT-1 splice variant glutamate transporter, has been found in case of human glaucoma and in a rat glaucoma model (Sullivan et al. 2006). However, despite these contradictory findings, the involvement of glutamate transporters of the retina in the pathogenesis of glaucoma cannot be excluded.

In this study, to clarify the involvement of the glutamate regulation system of the retina in the pathogenesis of glaucoma and to identify the specific glutamate transporters that are involved, we examined changes in the expression of two glutamate transporters, GLAST and GLT-1, by Western blot analysis and immunocytochemistry in a rat glaucoma model (Ju et al. 2006; Kim et al. 2007a, b; Park et al. 2007). This model is characterized by a moderate but chronic increase in the IOP, as is also observed in human primary open angle glaucoma.

Materials and methods

Animals

Eighty-four Sprague-Dawley rats (200–250 g) were used in accordance with the ARVO Statement regarding the Use of Animals in Ophthalmic and Vision Research. The Animal Care Committee of the Research Laboratory of Experimental Animals in the College of medicine at The Catholic University of Korea approved and monitored all the animal protocols. The animals were housed with a 14-h light/10-h dark cycle with standard chow and water *ad libitum*.

Experimental glaucoma

An elevated intraocular pressure (IOP) was induced in one eye in each of 78 animals [30 for immunocytochemistry, 36 for Western blot analysis, and 12 for counting retrogradely labeled retinal ganglion cells (RGCs)] by cauterizing the three episcleral veins. Briefly, the animals were anesthetized with chloral hydrate (400 mg/kg). After a conjunctival incision, the extraocular muscles were isolated and the four major limbal draining veins were identified based on their location, relative immobility, larger caliber, and branching pattern. Among them, the three episcleral veins were cauterized using a surgical microscope (Olympus, Tokyo, Japan), as described previously (Shareef et al. 1995). The other eye was used as the normal IOP control after sham surgery (conjunctival incisions with no cauterization) for the IOP comparison, immunocytochemistry, and Western blot analysis. One eye from six other rats that underwent sham operations was used as the normal IOP control for counting the retrograde labeled RGCs. A 30-inch tip was used to cauterize the vessels in an attempt to avoid possible damage to the neighboring sclera. Planar ophthalmoscopy was used to confirm the normal perfusion of the retina at an elevated IOP. Only those eyes that showed no evidence of scleral burns with subsequent necrosis or no complications after surgery were used in this study.

Retrograde labeling and counting of RGCs

The RGCs were retrogradely labeled 4 days before killing the animals by stereotaxically introducing Fluoro-Gold (Fluorochrome, Denver, CO, USA), either unilaterally or bilaterally, into the superior colliculus. Briefly, after fixing the head of the anesthetized rats in a stereotaxic apparatus (Stoelting, Wood Dale, IL, USA) with the skull held horizontally, the Fluoro-Gold tracer was injected into the superior colliculus using the following coordinates: 6 mm posterior to the rat bregma, 1.2 mm lateral to the midline, and 3.8–4.2 mm in depth from the top of the skull. These tracers are taken up by the axon terminals of RGCs in the superior colliculus and are transported retrogradely to the RGC somas in the retina. Immediately after killing, the superior side of each eye was marked to determine its orientation, and both eyes were enucleated. The anterior segments were removed and the posterior segments were fixed in 4% paraformaldehyde in 0.1 M phosphate buffer (PB), pH 7.4, for 30 min. The retina was

isolated, divided into four equal quadrants, and flat-mounted onto slides.

RGC counting was performed on the flat-mounted retinas from the normal IOP control ($n = 6$ retinas), and in animals 1 week ($n = 6$ retinas) and 6 weeks ($n = 6$ retinas) after elevating the IOP. The flat-mounted retinas were analyzed by fluorescent microscopy (Zeiss, Oberkochen, Germany). Each retinal quadrant was divided into central, middle, and peripheral locations (1, 2, and 3 mm from the optic disk, respectively). Labeled RGCs within a microscopic field of $200 \times 250\ \mu m^2$ were counted. Six microscopic fields of this size were used to count the RGCs in each quadrant. RGCs within the corresponding regions from each retina of the experimental and control groups were counted. For the statistical analysis, two different observers counted the RGCs in all four quadrants. The results were then averaged and are presented as the number of labeled RGCs. The data from the experimental and control groups were compared using the Student's t test, as described in the "Statistical analysis" subsection.

IOP measurements

The IOP was measured under topical anesthesia. An average of nine readings was recorded using a Tono-Pen XL tonometer (Solan, Florida, USA). Nine readings were carried out for each eye, and these were averaged to give a single measurement. The accuracy of the Tono-Pen readings, compared with other instruments, has been determined (Moore et al. 1993, 1995; Wirt et al. 1989). The IOP measurements were taken immediately before, 1 day after, and 3 days after surgery, and then weekly up to 6 weeks after surgery. At the same time, the IOPs of control eyes were measured. Only those eyes with Tono-Pen IOP values within the 95% confidence interval were used.

Tissue preparation

The experimental animals were killed by means of an overdose of chloral hydrate at the following times after surgery: 1 day, 3 days, 1, 2, 4, and 6 weeks for immunocytochemistry and Western blot analysis. For immunocytochemistry, the eyes were quickly enucleated and dissected, and the posterior eyecups were placed in a chilled fixative, 4% paraformaldehyde in 0.1 M PB (pH 7.4). The isolated retinas were divided into small pieces and immersion-fixed in the same fixative for 2 h at 4°C. After several washes, the fixed retinas were cryoprotected in 30% sucrose in 0.1 M PB for 6 h at 4°C. They were then stored in the same reagent at –70°C. For western blot analyses, the retinal tissues were quickly dissected, frozen in liquid nitrogen, and stored at –70°C.

Immunocytochemistry

The polyclonal rabbit anti-GLAST and anti-GLT-1 antibodies were generously donated by Dr. David Pow (University of Queensland). The specificity of both antibodies has already been tested (Pow et al. 2003). Small retinal pieces taken from the middle (~2 mm from the optic disk) of the inferior retina were pre-embedded in 3% agar in deionized water. Vibratome sections of 50-µm thickness were collected and washed several times in phosphate buffered saline (PBS). The sections were incubated in a blocking solution (10% normal donkey serum in PBS), followed by incubation with primary antibodies directed against GLAST and GLT-1 overnight at 4°C. The antibodies were diluted 1:1,000 for anti-GLAST and 1:500 for anti-GLT-1 in 0.1% Tween-20 in PBS. After the incubation, the sections were washed with PBS and incubated in rhodamine-conjugated anti-rabbit secondary antibodies purchased from Santa Cruz Biotechnology (SantaCruz, CA, USA) for 2 h. The sections were then washed and coverslipped. The stained sections were examined using a confocal microscope system (Bio-Rad, Hemel Hempstead, UK).

Image analysis

The method used in this experiment was modified from the previous method described by Wang et al. (2003). The intensity of immunoreactivity from photographs was analyzed using Image Pro®Plus 6.0 (Media Cybernetics Inc., Silver Spring, MD, USA). 450×400 µm fields on the same section as shown in Fig. 4 were measured and analyzed. Optical density data were corrected for background by subtracting the measurements. The intensity of labeling was determined automatically from whole areas of scanned retinal images by the computer program and gave a RGB value ranging from black to the incident level. Immunocytochemical parameters assessed in the area detected the mean integrated optical density; the mean integral calculus of the mean stained area times the intensity of the stain in each pixel in the area indicates the total amount of staining material in that area. Statistical analyses were performed using SPSS for Windows (version 11.0). Tests included the Student's t test, one-way analysis of variance (ANOVA), and Duncan's multiple comparison tests. Significance was considered at $P < 0.05$ and the data are presented as box plots.

Western blot analysis

The control retinas and retinas injured by chronic ocular hypertension were homogenized in RIPA buffer [1% Triton X-100, 5% SDS, 5% Deoxycholic acid, 0.5 M Tris–Cl (pH 7.5), 10% glycerol, 1 mM EDTA, 1 mM phenylmethylsulfonyl

fluoride (PMSF), 5 μg/ul aprotinin, 1 μg/ul leupeptin, 1 μg/ul pepstatin, 200 mM sodium orthovandates, and 200 mM sodium fluoride]. The tissue extracts were incubated on ice for 10 min, and clarified by centrifugation at 10,000*g* for 20 min at 4°C. The protein concentration in the total retina extracts was determined using a standard BCA assay (Pierce, Rockford, IL, USA). Thirty micrograms of retinal extract was resuspended at a 4:1 ratio into a 5 × sample buffer [60 mM Tris–HCl (pH 7.4), 25% glycerol, 2% SDS, 14.4 mM 2-mercaptoethanol, 0.1% bromophenol blue] that had been boiled for 4 min and resolved by SDS-PAGE. The proteins were then transferred to a nitrocellulose membrane (Hybond-C; Amersham Phamarcia Biotech, Freiburg, Germany), and the blots stained with Ponseau S (Sigma, St. Louis, MO, USA) to visualize the protein bands and to ensure that the protein loading was equal. The blots were washed and blocked for 1 h with a 5% solution of non-dried skim milk in TBST buffer [20 mM Tris–Cl pH 7.6, 137 mM NaCl, 0.1% Tween 20], and then incubated overnight with anti-GLAST and anti-GLT-1 antibodies (dilution 1:5,000). Finally, the blots were incubated with a 1:10,000 dilution of the peroxidase-conjugated goat anti-rabbit secondary antibodies. Detection accomplished by means of an enhanced chemiluminescence system (ECL, Amersham Pharmacia, CA, USA) and X-ray film development. The concentration of each transporter protein was determined using the ImageMaster VDS (Pharmacia Biotech, CA, USA). Optical densities (means ± SD) were obtained after four determinations for each experiment. The values of the experimental groups were compared with those from the control using a paired *t* test. Significance was set at $P < 0.05$.

Statistical analysis

The data are expressed as the mean ± SD. Comparisons between the two groups were performed using the Student's *t* test and a paired *t* test. Comparisons between multiple groups were performed using one-way ANOVA with Duncan's multiple pairwise comparison tests. The level of significance was set at $P < 0.05$.

Results

Experimental glaucoma

In this study, the IOP remained elevated for the entire 6-week experimental period without the need for any additional treatment. There were no infections or corneal lesions observed after the surgery. On the day of surgery (day 0), the IOP was 17.01 ± 1.59 mmHg in the cauterized eyes ($n = 75$) and 16.67 ± 1.81 mmHg in the normal control (contralateral) eyes ($n = 75$). The IOP gradually increased after surgery reaching 30.00 ± 1.48 mmHg ($n = 57$) 1 week after surgery. In contrast, the IOP in contralateral eyes was 16.40 ± 2.30 mmHg ($n = 57$). This elevated IOP in the case of the cauterized eyes was maintained for 6 weeks (32.50 ± 2.37 mmHg, $n = 15$). There were statistically significant differences in the IOP between the cauterized and contralateral sham operated eyes during the experimental period (Fig. 1).

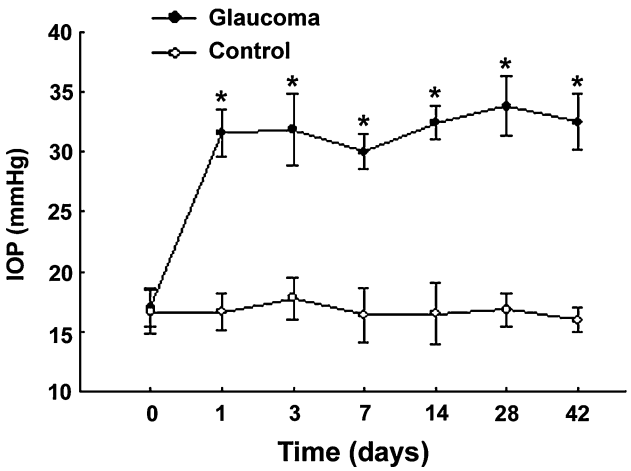

Fig. 1 Effect of chronic ocular hypertension on intraocular pressure (IOP; mean ± SD). The mean IOP of the eyes at 0, 1, 3 days, and 1, 2, 4 and 6 weeks after cauterizing the episcleral veins were 17.0, 31.6, 31.8, 30.0, 32.4, 33.8, and 32.5 mmHg respectively. Experimental glaucomatous eyes showed a significant and sustained increase in IOP during the experimental period: glaucoma, cauterized eye; control, not cauterized contralateral eye. *$P < 0.001$ compared with the control by a paired *t* test. *Error bars* represent standard deviation (SD)

Loss of RGCs after IOP elevation

Retrograde labeling of the RGCs was controlled for the rats' age in a previous study (Ju et al. 2006). Briefly, approximately 116,000 RGCs were counted in each retina (of the contralateral eye) at each experimental time point. No statistical difference was found between the eyes in these controls for up to 6 weeks after surgery. The ratio of the RGCs counted from the eyes of age-matched normal rats (aged 8 and 14 weeks, with normal IOP) to those of the control and the contralateral eyes of the experimental rats was 0.99 ± 0.23.

Whole-mounted paired retinas were prepared for the retrogradely labeled RGC observations and examined by fluorescence microscopy (Fig. 2). Table 1 summarizes RGC loss after cauterization. The average number of RGCs labeled with Fluoro-Gold in retinas ($n = 6$) of normal rat eyes was 113,779 ± 3,776 cells. This value was set to 100% when compared with the number of RGCs in the experimental group. Table 1 shows data concerning the

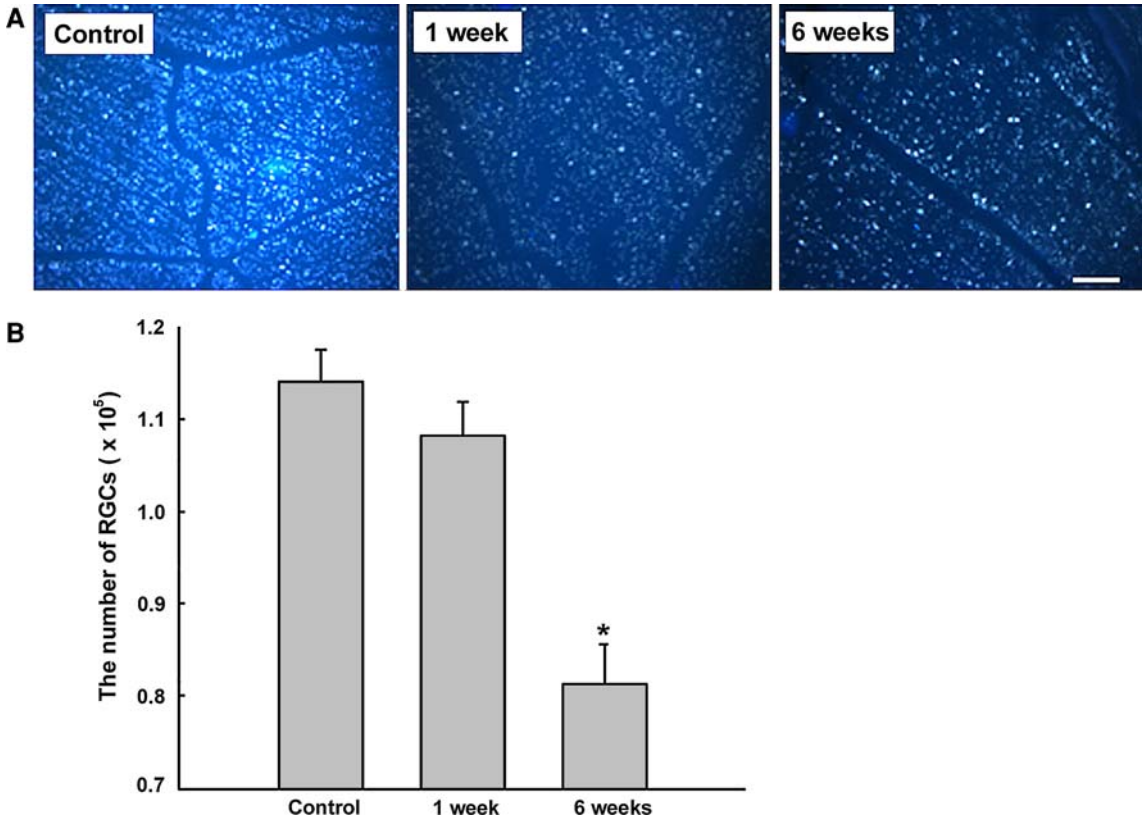

Fig. 2 Loss of retinal ganglion cells (RGCs) after cauterizing the episcleral veins. **a** Representative photomicrographs of flat-mount retinas from the superior temporal quadrant 1.5 mm from the optic disk, showing Fluoro-Gold-labeled RGCs in a control retina and cauterized retinas 1 and 6 weeks after surgery. **b** The counting of RGCs within a microscopic field of 200 × 250 μm^2 on flat-mounted retinas from the control ($n = 6$ retinas), and in animals 1 week ($n = 6$ retinas) and 6 weeks ($n = 6$ retinas) after cauterization. *Scale bar* 100 μm. *$P < 0.005$ compared with the control by a paired *t* test. *Error bars* represent SD

Table 1 Quantitative loss of RGCs after cauterization

Time after surgery	The number of RGCs	
	The number ± SD	Percentage
Control	113,779 ± 3,776	100
1 week	108,545 ± 3,641	95.4 ± 3.2
6 weeks	81,465 ± 4,437*	71.6 ± 3.9*

Values are reported as mean ± SD. The data were analyzed by Student's *t* test to determine the level of significance

* $P < 0.005$ compared with the control retina

quantitative loss of RGCs after chronic injury. 1 and 6 weeks after cauterization, the loss of RGCs in the central and peripheral regions of the retina from cauterized eyes relative to contralateral eyes was about 4.6 and 28.4%, respectively. Because the adult rat retina contains approximately 113,779 ± 3,776 RGCs, these results suggest that about 32,600 RGCs had degenerated during the 6 weeks after the initiation of chronic injury.

Western blot analysis for GLAST and GLT-1

Western blot analyses confirmed the presence of GLAST (59.7 kDa) and GLT-1 (63 kDa). Compared with the control eyes, the GLAST expression levels in cauterized eyes increased slightly during the experimental period, whereas the GLT-1 expression level increased significantly (Fig. 3a). Densitometric analysis showed that there were no statistically significant differences in the level of GLAST expression in the cauterized retina. In contrast, GLT-1 expression in the cauterized retinas continued to increase after 1 week, and peaked at 6 weeks at a level nine times higher than the control retinas (Fig. 3b).

Immunocytochemistry for GLT-1 and GLAST

GLT-1 expression was detected in the outer nuclear layer (ONL), the outer plexiform layer (OPL), the inner nuclear layer (INL), and the inner plexiform layer (IPL) of control and injured retinas. Based on the morphology of the labeled somata and emerging processes, GLT-1 immunoreactive

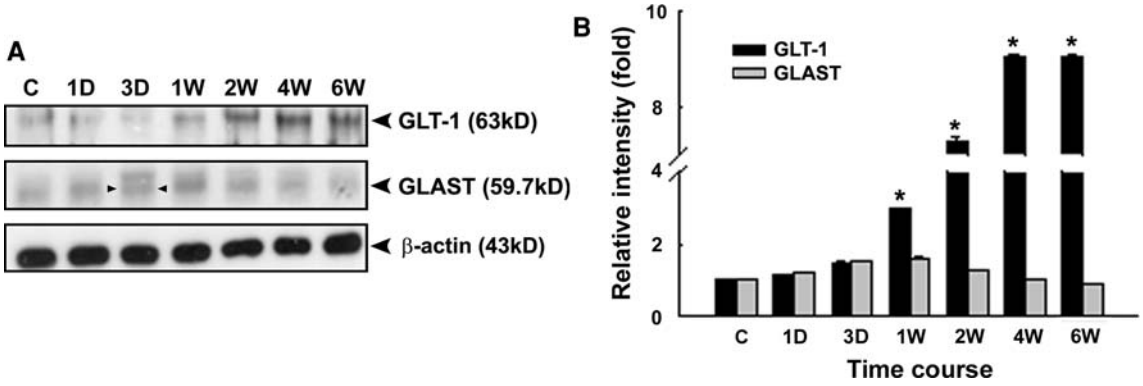

Fig. 3 Immunoblotting analysis of glutamate transporters. **a** Representative immunoblots for GLT-1 and GLAST from control and cauterized retina at days 1 and 3, and at weeks 1, 2, 4 and 6. In the 3 days of the GLAST Western blot, two bands are evident. The *lower band* (*arrowheads*) indicates the GLAST (Williams et al. 2005). **b** Quantification of the relative expression of GLT-1 and GLAST (mean ± SD). The relative intensity on the normal IOP retina is considered to be one-fold: *C* control, normal IOP retina. **P* < 0.001 compared with control

cells were easily identified as cone photoreceptors and a subset of cone bipolar cells. The GLT-1 expression patterns of glaucomatous retinas throughout the entire experimental period were quite similar to that in control retinas. Three days after cauterization, however, the intensity of the GLT-1 immunoreactivity appeared to increase throughout the entire experimental period and peaked at 6 weeks after injury (Fig. 4a).

GLAST immunoreactivity was diffuse in the control retinas, from the innermost to the outermost part of the retina, including GCL, IPL, and OPL. This pattern and expression of GLAST expression in cauterized retinas was similar to that of control retina throughout the entire experimental period (Fig. 4b).

Image analysis

We quantitatively analyzed the immunocytochemistry results for changes in GLT-1 and GLAST expression during the experimental periods. The optical densities were measured from the images shown in Fig. 4a, b, by using an image analysis program, and the data were statistically analyzed. Figure 4c shows box plots for the strength of GLT-1 and GLAST immunolabeling. As shown in the box plots, GLT-1 expression tended to increase with increasing time, and the GLAST expression was featureless. A statistical analysis indicated significant differences in the level of GLT-1 expression in the retinas 4 and 6 weeks after cauterization ($P < 0.05$) and in the level of GLAST expression in the retinas at 3 days, 1 week and 6 weeks after cauterization ($P < 0.05$).

Discussion

If excessive glutamate in the retina plays a role in glaucomatous optic neuropathy through excitotoxicity, as has been proposed, it is possible that a perturbed retinal glutamate homeostasis system could be responsible for this pathogenesis. In light of these proposals, we examined changes in the expression of two glutamate transporters, GLAST and GLT-1, by Western blot analysis and immunocytochemistry in a rat glaucoma model characterized by a moderate but chronic increase in the IOP.

In the present study, we calculated RGC numbers in normal and experimental groups using retrograde labeling with Fluoro-Gold, in order to evaluate an experimental model of glaucoma which is characterized by retinal ganglion cell loss. In control retinas, the number of RGCs was 113,779 and of these, 32,600 RGCs had degenerated during the 6-week period after the chronic increase in IOP. This suggests that our experimental glaucoma model reflects a cardinal characteristic of glaucoma. However, the numbers of RGCs were smaller than those recently reported by Salinas-Navarro et al. (2009), who reported a total of 82,000 RGCs. This discrepancy could be due to the methods employed to estimate the total RGC population.

In the present study, GLT-1 expression was increased in cauterized eyes throughout the entire experimental period, statistically significant in retinas 4 and 6 weeks after cauterization. In case of GLAST expression, although statistical image analysis of GLAST immunohistochemistry demonstrated decrease in the level of GLAST expression in the retinas at 6 weeks after cauterization ($P < 0.05$), we concluded no consistent change during the experimental period, because the expression pattern of GLAST fluctuated during experimental period and the levels of GLAST expression at 2 and 4 weeks after cauterization were similar to that in normal control. These results differ from previous reports that GLAST levels were reduced in rat (Martin et al. 2002) and mouse models of glaucoma (Schuettauf et al. 2007) and in human glaucoma (Naskar et al. 2000), where GLAST levels increased time-dependently, reaching a

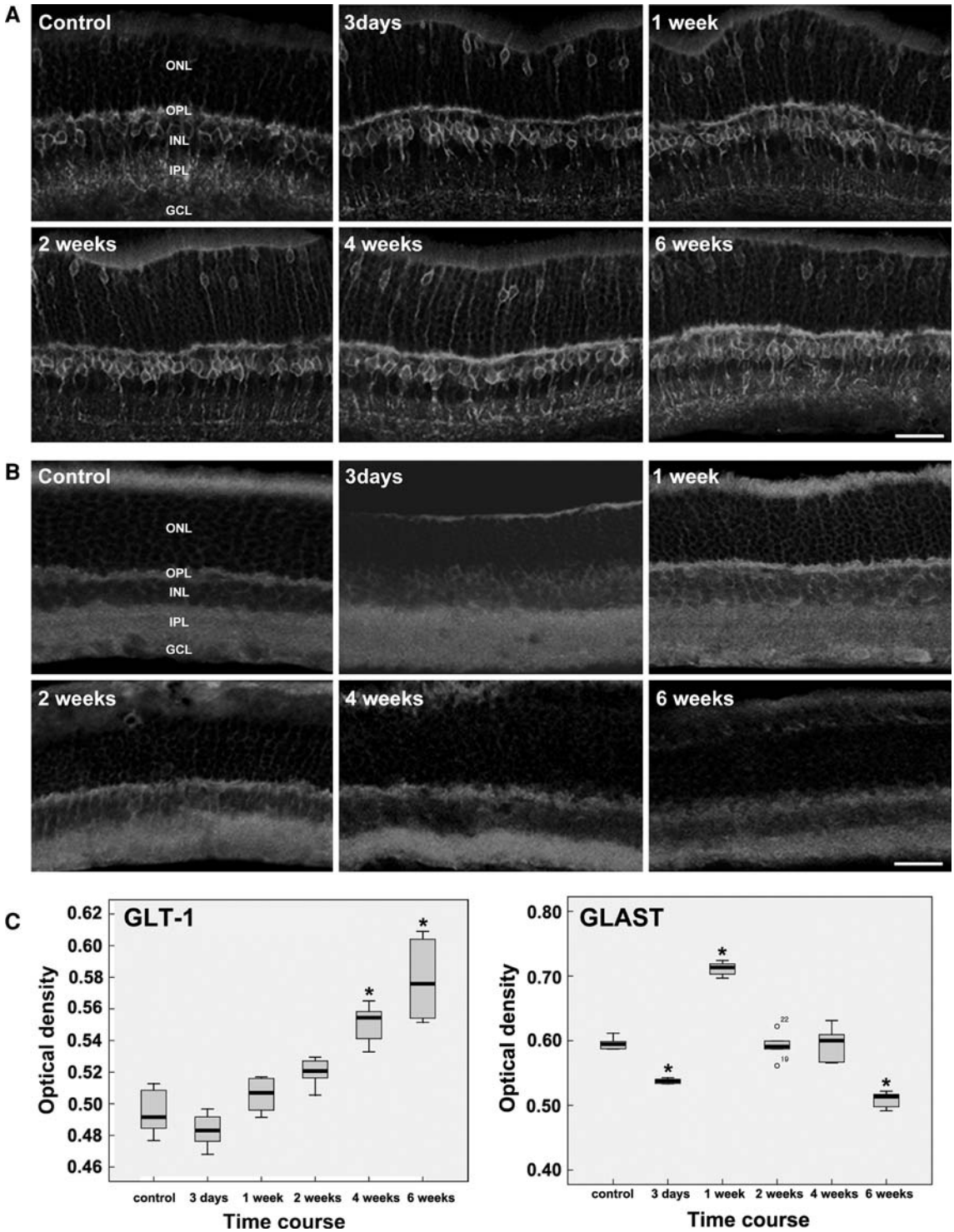

Fig. 4 Cellular distribution of the glutamate transporter, GLT-1 (**a**) and GLAST (**b**), after inducing chronic ocular hypertension. **a** In the control retina, GLT-1 immunoreactivity was observed in cone bipolar cells and faintly in cone photoreceptor cells. After episcleral vein cauterization, GLT-1 immunoreactivity increased significantly for 6 weeks and the synaptic configurations between photoreceptor and bipolar cells were clearly identified. **b** Cellular localization and GLAST expression in the rat retina following chronic injury. The pattern of GLAST expression appeared to be similar to that of the controls. *Scale bar* 50 μm. *GCL* ganglion cell layer; *INL* inner nuclear layer; *ONL* outer nuclear layer. **c** Image analysis for immunocytochemistry results for GLT-1 and GLAST shown in **a** and **b**, respectively. Data are presented as *vertical box plots*. A *box* parallel with the *numbered line* bounded on the *bottom* by the first quartile ($\chi_{0.25}$) and on the *top* by the third quartile ($\chi_{0.75}$). A *strong line* inside the *box* denotes the median value. Any data observation that was lower than 1.5 the first quartile or higher than 1.5 the third quartile is considered to constitute an outlier and is indicated as *degree symbol*, and a non-outlier observation represents as *bar*. *$P < 0.05$ compared with the control

maximum after 3 weeks of an elevated IOP in a rat glaucoma model (Woldemussie et al. 2004), and that GLT-1 was down-regulated in glaucomatous eyes in rats (Martin et al. 2002) and mice (Schuettauf et al. 2007). These discrepancies might be mainly caused by the differences in the antibodies and glaucoma model. That is, antibodies against GLT-1 used by Martin et al. (2002) did not label cone photoreceptors and any cone bipolar cells, while our antibodies clearly labeled them. DBA/2J mouse, which has been used as a closed-angle glaucoma model, was used by Schuettauf et al. (2007), whereas rat episcleral vein cauterization model, which has been considered as an open-angle glaucoma model, was used in this study. The differences in species and experimental procedures might also affect different results.

GLAST and GLT-1 are dominant types among the five known glutamate transporters in the brain and are coexpressed in astrocytes (Danbolt et al. 1992; Lehre et al. 1995; Levy et al. 1993). The selective in vivo knockout of individual glutamate transporters has shown that the astroglial uptake of glutamate by GLT-1 and GLAST is a major mechanism in excitotoxicity and the clearance of glutamate in the brain (Rothstein et al. 1996). In the retina, Müller cells are counterparts of astrocytes in the brain. This main type of glial cell in the retina plays a primary role in glutamate uptake and is involved in various pathological conditions in the retina, including glaucoma (Bringmann et al. 2006). In contrast to the astrocytes of the brain, Müller cells only express GLAST (Izumi et al. 2002; Pow 2001; Rauen 2000; Rauen et al. 1996, 1998), while GLT-1 is expressed in retinal neurons, cone photoreceptors and certain types of cone bipolar cells (Pow 2001; Rauen 2000; Rauen et al. 1996). This suggests that GLAST is the most important glutamate transporter for maintaining glutamate homeostasis in the retina.

However, our results and recent results reported by other investigators (Martin et al. 2002; Naskar et al. 2000; Schuettauf et al. 2007), as mentioned above, have demonstrated that GLAST expression remains stable or decreases in the retina of glaucomatous eyes. This suggests that GLAST might not be the primary glutamate transporter for maintaining glutamate homeostasis in pathological conditions, such as glaucoma. In contrast, GLT-1 appears to play an active role in the maintenance of glutamate homeostasis in the retina of glaucomatous eyes, and thus GLT-1 may be the major factor in maintaining glutamate homeostasis in pathological conditions. This hypothesis is reasonable for the following reasons: (1) GLT-1 contributes more largely to the maintenance of tonic cerebrospinal glutamate concentration in the brain than GLAST (Rothstein et al. 1996). (2) GLT-1 plays a major role and is responsible for up to 90% of all glutamate transport in the forebrain region (Robinson 1998). (3) Exogenous treatment with subtype-specific antisense oligonucleotides to GLT-1 led to an increase in vitreous glutamate and RGC death in rats (Vorwerk et al. 2000). (4) Recently, the evoked expression of GLT-1c, a GLT-1 splice variant glutamate transporter, has been found in human glaucoma and in a rat glaucoma model (Sullivan et al. 2006). The results reported herein also show that GLT-1 expression is significantly increased in another rat model of glaucoma which is induced by cauterizing the three episcleral veins. Therefore, GLT-1 may play an important role in the maintenance of glutamate homeostasis in the retina undergoing glaucoma.

However, the possibility that GLAST is the primary regulator of glutamate in the retina and that the dysfunction of GLAST in Müller cells is the main cause of glaucoma cannot be excluded. Despite this, the findings that dynamic changes in GLT-1 expression occur in models of glaucoma clearly indicate that GLT-1 may be a prerequisite for the maintenance of glutamate homeostasis in the retina undergoing glaucoma.

Acknowledgment This work was supported by the Catholic Medical Center Research Foundation (S. C. Park) and a Korea Research Foundation Grant (KRF-2007-313-E00007) from the Korean Government (I.-B. Kim).

References

Arriza JL, Eliasof S, Kavanaugh MP, Amara SG (1997) Excitatory amino acid transporter 5, a retinal glutamate transporter coupled to a chloride conductance. Proc Natl Acad Sci USA 94:4155–4160

Bringmann A, Pannicke T, Grosche J, Francke M, Wiedermann P, Skatchkov SN, Osborne NN, Reichenbach A (2006) Müller cells in the healthy and diseased retina. Prog Retin Eye Res 25:397–424

Danbolt NC (2001) Glutamate uptake. Prog Neurobiol 65:1–105

Danbolt NC, Storm-Mathisen J, Kanner BI (1992) An [Na^+ + K^+] coupled L-glutamate transporter purified from rat brain is located in glial cell processes. Neuroscience 51:295–310

Dreyer EB, Zurakowski D, Schumer RA, Podos SM, Lipton SA (1996) Elevated glutamate levels in the vitreous body of humans and monkeys with glaucoma. Arch Ophthalmol 114:299–305

Fairman WA, Vandenberg RJ, Arriza JL, Kavanaugh MP, Amara SG (1995) An excitatory amino-acid transporter with properties of a ligand-gated chloride channel. Nature 375:599–603

Izumi Y, Shimamoto K, Benz AM, Hammerman SB, Olney JW, Zorumski CF (2002) Glutamate transporters and retinal excitotoxicity. Glia 39:58–68

Ju KR, Kim HS, Kim JH, Lee NY, Park CK (2006) Retinal glial cell responses and Fas/FasL activation in rats with chronic ocular hypertension. Brain Res 1122:209–221

Kanai Y, Hediger MA (1992) Primary structure and functional characterization of a high-affinity glutamate transporter. Nature 360:467–471

Kim HS, Chang YI, Kim JH, Park CK (2007a) Alteration of retinal intrinsic survival signal and effect of alpha2-adrenergic receptor agonist in the retina of the chronic ocular hypertension rat. Vis Neurosci 24:127–139

Kim JH, Lee NY, Jung SW, Park CK (2007b) Expression of N-methyl-d-aspartate receptor 1 in rats with chronic ocular hypertension. Neuroscience 149:908–916

Lehre KP, Levy LM, Ottersen OP, Storm-Mathisen J, Danbolt NC (1995) Differential expression of two glial glutamate transporters in the rat brain: quantitative and immunocytochemical observations. J Neurosci 15:1835–1853

Lehre KP, Davanger S, Danbolt NC (1997) Localization of the glutamate transporter protein GLAST in rat retina. Brain Res 744:129–137

Levy LM, Lehre KP, Rolstad B, Danbolt NC (1993) A monoclonal antibody raised against an [$Na^+ + K^+$] coupled L-glutamate transporter purified from rat brain confirms glial cell localization. FEBS Lett 317:79–84

Maragakis NJ, Rothstein JD (2001) Glutamate transporters in neurologic disease. Arch Neurol 58:365–370

Martin KR, Levkovitch-Verbin H, Valenta D, Baumrind L, Pease ME, Quigley HA (2002) Retinal glutamate transporter changes in experimental glaucoma and after optic nerve transection in the rat. Invest Ophthalmol Vis Sci 43:2236–2243

Massey SC, Miller RF (1990) N-methyl-D-aspartate receptors of ganglion cells in rabbit retina. J Neurophysiol 63:16–30

Moore CG, Milne ST, Morrison JC (1993) Noninvasive measurement of rat intraocular pressure with the Tono-Pen. Invest Ophthalmol Vis Sci 34:363–369

Moore CG, Epley D, Milne ST, Morrison JC (1995) Long-term noninvasive measurement of intraocular pressure in the rat eye. Curr Eye Res 14:711–717

Naskar R, Vorwerk CK, Dreyer EB (2000) Concurrent downregulation of a glutamate transporter and receptor in glaucoma. Invest Ophthalmol Vis Sci 41:1940–1944

Park SH, Kim JH, Kim YH, Park CH (2007) Expression of neuronal nitric oxide synthase in the retina of a rat model of chronic glaucoma. Vis Res 47:2732–2740

Pines G, Danbolt NC, Bjørås M, Zhang Y, Bendahan A, Eide L, Koepsell H, Storm-Mathisen J, Seeberg E, Kanner BI (1992) Cloning and expression of a rat brain L-glutamate transporter. Nature 360:464–467

Pow DV (2001) Amino acids and their transporters in the retina. Neurochem Int 38:463–484

Pow DV, Barnett NL (2000) Developmental expression of excitatory amino acid transporter 5: a photoreceptor and bipolar cell glutamate transporter in rat retina. Neurosci Lett 280:21–24

Pow DV, Sullivan R, Scott H (2003) Antibody production and immunocytochemical localization of amino acid transporters. Methods Mol Biol 227:213–244

Rauen T (2000) Diversity of glutamate transporter expression and function in the mammalian retina. Amino Acids 19:53–62

Rauen T, Rothstein JD, Wässle H (1996) Differential expression of three glutamate transporter subtypes in the rat retina. Cell Tissue Res 286:325–336

Rauen T, Taylor WR, Kuhlbrodt K, Wiessner M (1998) High-affinity glutamate transporters in the rat retina: a major role of the glial glutamate transporter GLAST-1 in transmitter clearance. Cell Tissue Res 291:19–31

Robinson MB (1998) The family of sodium-dependent glutamate transporters: a focus on the GLT-1/EAAT2 subtype. Neurochem Int 33:479–491

Rothstein JD, Martin LJ, Kuncl RW (1992) Decreased glutamate transport by the brain and spinal cord in amyotrophic lateral sclerosis. N Engl J Med 326:1464–1468

Rothstein JD, Dykes-Hoberg M, Pardo CA, Bristol LA, Jin L, Kuncl RW, Kanai Y, Hediger MA, Wang Y, Schielke JP, Welty DF (1996) Knockout of glutamate transporters reveals a major role for astroglial transport in excitotoxicity and clearance of glutamate. Neuron 16:675–686

Salinas-Navarro M, Mayor-Torroglosa S, Jiménz-López M, Avilés-Trigueros M, Holmes TM, Lund RD, Villegas-Pérez MP, Vidal-Sanz M (2009) A computerized analysis of the entire retinal ganglion cell population and its spatial distribution in adult rats. Vision Res 49:115–126

Schuettauf F, Thaler S, Bolz S, Fries J, Kalbacher H, Mankowska A, Zurakowski D, Zrenner E, Rejdak R (2007) Alterations of amino acids and glutamate transport in the DBA/2J mouse retina; possible clues to degeneration. Graefes Arch Clin Exp Ophthalmol 245:1157–1168

Shareef SR, Garcia-Valenzuela E, Salierno A, Walsh J, Sharma SC (1995) Chronic ocular hypertension following episcleral venous occlusion in rats. Exp Eye Res 61:379–382

Storck T, Schulte S, Hofmann K, Stoffel W (1992) Structure, expression, and functional analysis of a Na^+-dependent glutamate/aspartate transporter from rat brain. Proc Natl Acad Sci USA 89:10955–10959

Sullivan RK, Woldemussie E, Macnab L, Ruiz G, Pow DV (2006) Evoked expression of the glutamate transporter GLT-1c in retinal ganglion cells in human glaucoma and in a rat model. Invest Ophthalmol Vis Sci 47:3853–3859

Vorwerk CK, Naskar R, Schuettauf F, Quinto K, Zurakowski D, Gochenauer G, Robinson MB, Mackler SA, Dreyer EB (2000) Depression of retinal glutamate transporter function leads to elevated intravitreal glutamate levels and ganglion cell death. Invest Ophthalmol Vis Sci 41:3615–3621

Wang Q, Zeng YJ, Huo P, Hu JL, Zhang JH (2003) A specialized plug-in software module for computer-aided quantitative measurement of medical images. Med Eng Phys 25:887–892

Williams SM, Sullivan RKP, Scott HL, Finkelstein DI, Colditz PB, Lingwood BE, Dodd PR, Pow DV (2005) Glial glutamate transporter expression patterns in brains from multiple mammalian species. Glia 49:520–541

Wirt H, Draeger J, Rumberger E, Deutsch C, Dauper J (1989) Comparative studies of the calibration of new electronic automatic tonometers. Fortschr Ophthalmol 86:403–406

Woldemussie E, Wijono M, Ruiz G (2004) Muller cell response to laser-induced increase in intraocular pressure in rats. Glia 47:109–119